



Cocaine Disinhibits Dopamine Neurons by Potentiation of GABA Transmission in the Ventral Tegmental Area

Christina Bocklisch *et al.*
Science **341**, 1521 (2013);
DOI: 10.1126/science.1237059

This copy is for your personal, non-commercial use only.

If you wish to distribute this article to others, you can order high-quality copies for your colleagues, clients, or customers by [clicking here](#).

Permission to republish or repurpose articles or portions of articles can be obtained by following the guidelines [here](#).

The following resources related to this article are available online at www.sciencemag.org (this information is current as of May 19, 2014):

Updated information and services, including high-resolution figures, can be found in the online version of this article at:

<http://www.sciencemag.org/content/341/6153/1521.full.html>

Supporting Online Material can be found at:

<http://www.sciencemag.org/content/suppl/2013/09/25/341.6153.1521.DC1.html>

A list of selected additional articles on the Science Web sites **related to this article** can be found at:

<http://www.sciencemag.org/content/341/6153/1521.full.html#related>

This article **cites 33 articles**, 10 of which can be accessed free:

<http://www.sciencemag.org/content/341/6153/1521.full.html#ref-list-1>

This article has been **cited by 2 articles** hosted by HighWire Press; see:

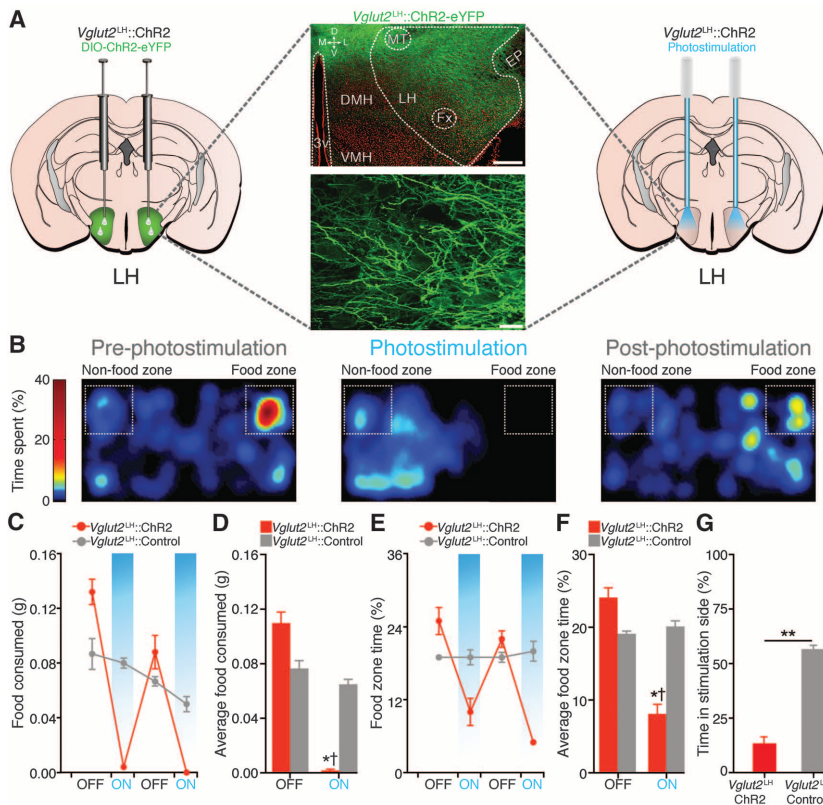
<http://www.sciencemag.org/content/341/6153/1521.full.html#related-urls>

This article appears in the following **subject collections**:

Neuroscience

<http://www.sciencemag.org/cgi/collection/neuroscience>

Fig. 4. Photoactivation of *Vglut2*^{LH} neurons suppresses feeding in food-deprived mice and is aversive. (A) ChR2-eYFP expression in the LH of a *Vglut2-ires-Cre* mouse. Scale bars, 200 μ m (top), 20 μ m (bottom). (B) Spatial location heat maps in 10-min epochs before, during, and after 5-Hz photostimulation. (C and D) Photostimulation of *Vglut2*^{LH} neurons significantly decreased food intake ($F_{1,36} = 13.31, P < 0.001$) and food zone time (E and F) ($F_{1,36} = 13.12, P < 0.001, n = 5$ mice per group). (G) *Vglut2*^{LH}::ChR2 mice spent significantly less time in the photostimulation-paired side when compared with controls ($P < 0.001, n = 5$ mice per group).



References and Notes

- B. G. Hoebel, P. Teitelbaum, *Science* **135**, 375–377 (1962).
- J. M. Delgado, B. K. Anand, *Am. J. Physiol.* **172**, 162–168 (1953).
- R. A. Wise, *Science* **162**, 377–379 (1968).
- B. G. Stanley, L. H. Ha, L. C. Spears, M. G. Dee II, *Brain Res.* **613**, 88–95 (1993).
- C. I. Turenius et al., *Brain Res.* **1262**, 16–24 (2009).
- J. D. Hahn, L. W. Swanson, *J. Comp. Neurol.* **520**, 1831–1890 (2012).
- J. S. de Olmos, L. Heimer, *Ann. N.Y. Acad. Sci.* **877**, 1–32 (1999).
- J. H. Jennings et al., *Nature* **496**, 224–228 (2013).
- S.-Y. Kim et al., *Nature* **496**, 219–223 (2013).
- T. Kudo et al., *J. Neurosci.* **32**, 18035–18046 (2012).
- M. Angeles-Castellanos, J. Mendoza, C. Escobar, *Neuroscience* **144**, 344–355 (2007).
- P. M. Johnson, P. J. Kenny, *Nat. Neurosci.* **13**, 635–641 (2010).
- B. Y. Chow et al., *Nature* **463**, 98–102 (2010).
- J. Mattis et al., *Nat. Methods* **9**, 159–172 (2011).
- M. M. Karmani, G. Szabó, F. Erdélyi, D. Burdakov, *J. Physiol.* **591**, 933–953 (2013).
- Z. A. Knight et al., *Cell* **151**, 1126–1137 (2012).
- G. M. Leininger et al., *Cell Metab.* **14**, 313–323 (2011).
- T. Sakurai et al., *Cell* **92**, 573–585 (1998).
- R. Sharf et al., *Biol. Psychiatry* **67**, 753–760 (2010).
- L. W. Swanson, G. Sanchez-Watts, A. G. Watts, *Neurosci. Lett.* **387**, 80–84 (2005).
- D. Atasoy, J. N. Betley, H. H. Su, S. M. Sternson, *Nature* **488**, 172–177 (2012).
- H.-R. Berthoud, H. Münzberg, *Physiol. Behav.* **104**, 29–39 (2011).
- M. Watabe-Uchida, L. Zhu, S. K. Ogawa, A. Vamanrao, N. Uchida, *Neuron* **74**, 858–873 (2012).
- I. R. Wickersham, S. Finke, K.-K. Conzelmann, E. M. Callaway, *Nat. Methods* **4**, 47–49 (2007).
- J. Olds, P. Milner, *J. Comp. Physiol. Psychol.* **47**, 419–427 (1954).

Acknowledgments: We thank the Stuber laboratory and C. Bulik for discussion. We thank K. Deisseroth and E. Boyden for viral constructs and the University of

North Carolina (UNC) Vector Core for viral packaging, B. Lowell and L. Vogt for mice, and the UNC Neuroscience Center Microscopy Core (P30 NS045892). This study was supported by the Klarman Family Foundation, the Brain and Behavior Research Foundation, the Foundation of Hope, and the National Institute on Drug Abuse (DA032750) and the National Institute on Alcohol Abuse and Alcoholism (AA022234 and AA011605). A.M.S. was supported by NS007431 and DA034472.

Supplementary Materials

www.sciencemag.org/content/341/6153/1517/suppl/DC1
Materials and Methods
Figs. S1 to S13
Tables S1 and S2
Movie S1
References (26, 27)

12 June 2013; accepted 28 August 2013
10.1126/science.1241812

Cocaine Disinhibits Dopamine Neurons by Potentiation of GABA Transmission in the Ventral Tegmental Area

Christina Bocklisch,^{1*} Vincent Pascoli,¹ Jovi C. Y. Wong,^{1†} David R. C. House,¹ Cédric Yvon,¹ Mathias de Roo,¹ Kelly R. Tan,¹ Christian Lüscher^{1,2‡}

Drug-evoked synaptic plasticity in the mesolimbic system reshapes circuit function and drives drug-adaptive behavior. Much research has focused on excitatory transmission in the ventral tegmental area (VTA) and the nucleus accumbens (NAc). How drug-evoked synaptic plasticity of inhibitory transmission affects circuit adaptations remains unknown. We found that medium spiny neurons expressing dopamine (DA) receptor type 1 (D1R-MSNs) of the NAc project to the VTA, strongly preferring the GABA neurons of the VTA. Repeated *in vivo* exposure to cocaine evoked synaptic potentiation at this synapse, occluding homosynaptic inhibitory long-term potentiation. The activity of the VTA GABA neurons was thus reduced and DA neurons were disinhibited. Cocaine-evoked potentiation of GABA release from D1R-MSNs affected drug-adaptive behavior, which identifies these neurons as a promising target for novel addiction treatments.

Disinhibition, the removal of an inhibitory brake on neuronal firing, may affect circuit function in several parts of the brain (1–3). Disinhibition of ventral tegmental area (VTA) DA neurons has been implicated in drug reinforcement when, in the acute phase, the addictive

drug shuts down VTA γ -aminobutyric acid (GABA) neurons (4–6). To understand how this monosynaptic building block integrates into the larger circuitry, we characterized the functional anatomy

of the inhibitory projections to the VTA. We focused on the major input that originates in the nucleus accumbens (NAc). Accumbal medium spiny neurons (MSNs) fall into two classes, the D1R-MSNs and D2R-MSNs (7), which may segregate with the projection target. To reveal the type of MSN projecting to the midbrain, we injected a retrograde tracer (B subunit of cholera toxin) fused to a fluorescent cyanine dye (CTB-Cy3) into the VTA of bacterial artificial chromosome (BAC) transgenic mice in which the expression of enhanced green fluorescent protein (EGFP) is driven by the promoters of D1 or D2 receptors, respectively (D1R-EGFP and D2R-EGFP mice; Fig. 1A). We then counted the CTB-Cy3–

positive cells and determined the colocalization with EGFP in neurons of the NAc of both mouse lines (Fig. 1B; Hoechst, a nuclear stain, was used to obtain the total number of cells, $n = 1721$ and $n = 1922$ in D1R-EGFP and D2R-EGFP mice, respectively; 3 animals each). EGFP-positive cells accounted for about half of all cells (D1R-mice, $52 \pm 2\%$; D2R-EGFP mice, $43 \pm 1\%$; Fig. 1C). A smaller fraction of cells, similar in both mouse lines, was positive for CTB-Cy3 (D1R-EGFP mice, $34 \pm 8\%$; D2R-EGFP mice, $33 \pm 4\%$; Fig. 1C). Colocalization with EGFP was observed only in D1R-EGFP mice (Fig. 1, B and C). Hence, only D1R-MSNs project directly to the midbrain.

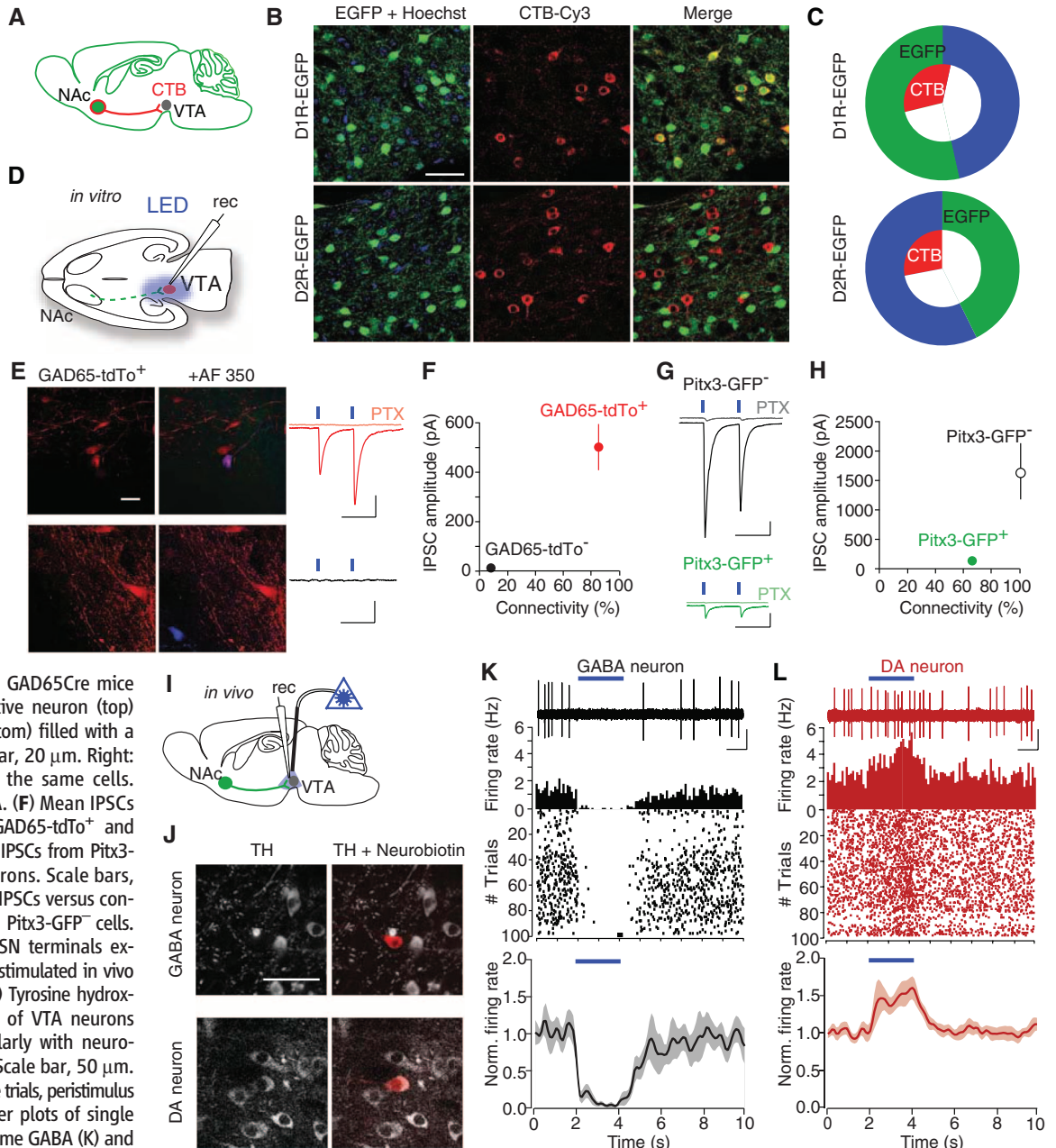
¹Department of Basic Neurosciences, Medical Faculty, University of Geneva, CH-1211 Geneva, Switzerland. ²Clinic of Neurology, Department of Clinical Neurosciences, Geneva University Hospital, CH-1211 Geneva, Switzerland.

*Present address: NWFZ, Charite Universitätsmedizin, Chariteplatz 1, 10117 Berlin, Germany.

†Present address: Nuffield Laboratory of Ophthalmology, Nuffield Department of Clinical Neurosciences, University of Oxford, Oxford OX3 9DU, UK.

‡Corresponding author. E-mail: christian.luscher@unige.ch

Fig. 1. VTA-projecting MSNs express D1Rs and disinhibit VTA DA neurons in vivo by preferentially targeting VTA GABA neurons. (A) Experimental setup: Injection of retrograde tracer CTB-Cy3 into the VTA of D1R- or D2R-EGFP mice. (B) Confocal images of NAc slices from D1R-EGFP⁺ or D2R-EGFP⁺ mice (green) injected intra-VTA with CTB-Cy3 (red). Scale bar, 50 μ m. (C) EGFP⁺ (green) neurons and CTB-Cy3-labeled cells (red) as a proportion of total cell number (blue) in each mouse line. Overlapping segments represent colocalization. (D) In vitro slices. Chr2-Venus was expressed in the NAc of GAD65Cre-tdTo or Pitx3-GFP mice and VTA-projecting MSN terminals were stimulated with blue light. (E) Images of VTA slices from GAD65Cre mice showing a tdTomato-positive neuron (top) and negative neuron (bottom) filled with a blue dye (AF 350). Scale bar, 20 μ m. Right: Whole-cell recordings of the same cells. Scale bars, 50 ms, 100 pA. (F) Mean IPSCs versus connectivity of GAD65-tdTo⁺ and GAD65-tdTo⁻ neurons. (G) IPSCs from Pitx3-GFP⁻ and Pitx3-GFP⁺ neurons. Scale bars, 50 ms, 200 pA. (H) Mean IPSCs versus connectivity of Pitx3-GFP⁺ and Pitx3-GFP⁻ cells. (I) Experimental setup: MSN terminals expressing Chr2-Venus were stimulated in vivo by illuminating the VTA. (J) Tyrosine hydroxylase (TH, white) staining of VTA neurons labeled in vivo juxtacellularly with neurobiotin (red, right panels). Scale bar, 50 μ m. (K and L) Top: Representative trials, peristimulus time histograms, and raster plots of single unit recordings from the same GABA (K) and DA neuron (L) shown in (J). Blue bar denotes a 2-s laser pulse. Scale bars, 1 s, 10 mV. Bottom: Average normalized firing rates during blue laser stimulation of GABA neurons (K) and DA neurons (L) identified with juxtacellular labeling. All data are means \pm SEM.



Because the VTA contains GABA and DA neurons (8) and because recent studies have suggested that MSNs of the NAc project to both (9, 10), we aimed to characterize the functional connectivity between MSNs and VTA neurons. We expressed ChR2 in the NAc of mice that expressed a fluorescent marker in VTA GABA neurons (GAD65-tdTomato) and prepared acute slices of the VTA (Fig. 1D). We recorded from both tdTomato⁺ and tdTomato⁻ neurons (Fig. 1E) and induced GABA release by wide-field illumination. Large inhibitory postsynaptic currents (IPSCs) were elicited in the majority (87.4%) of tdTomato⁺ neurons (497 ± 89 pA, $n = 17$), whereas only a small fraction of tdTomato⁻ neurons was responsive (8.3%, 20.3 ± 15.2 pA, $n = 24$; Fig. 1F). Both picrotoxin (PTX, 100 μ M, $n = 5$) and tetrodotoxin (TTX, 0.5 μ M, $n = 5$; Fig. S1) abolished the IPSCs in tdTomato⁺ neurons, confirming action potential-dependent transmitter release followed by GABA_A receptor activation (Fig. 1E). Clearly, accumbal MSNs exert strong inhibition onto VTA GABA neurons. To reveal a possible functionally weaker connectivity onto DA neurons, we expressed the more efficient ChR2(H134R) (11) into the NAc of Pitx3-GFP mice (a marker for DA neurons) (12). Under these circumstances, we detected small IPSCs in 67% of the Pitx3-GFP⁺ cells (127 ± 44 pA, $n = 12$) and large IPSCs in 100% of Pitx3-GFP⁺ neurons (1602 ± 473 pA, $n = 10$; Fig. 1, G and H). Thus, although a direct inhibitory projection onto VTA DA neurons exists (10), we found a much more frequent and stronger inhibitory connection onto VTA GABA cells (9). This suggested that D1R-MSNs of the NAc could drive disinhibition of VTA DA neurons (13).

We therefore performed *in vivo* single unit recordings of VTA neurons in response to optical stimulation of MSN terminals in the VTA in anaesthetized mice (Fig. 1I). We first recorded from GABA neurons, as confirmed by juxtacellular

labeling methods and post hoc immunohistochemistry (Fig. 1J, top). All GABA neurons responded to a 2-s light pulse with decreased spiking activity ($-92.2 \pm 2\%$ of baseline activity, $n = 4$; Fig. 1K). We next recorded from DA neurons (Fig. 1J, bottom), whose activity was increased when the blue light was flashed ($146.8 \pm 10.5\%$ of baseline, $n = 7$, $P < 0.05$; Fig. 1L). Thus, despite a weak direct inhibitory connection to VTA DA neurons, D1R-MSN terminal activation leads to their disinhibition. This scenario was confirmed when we expressed the inhibitory opsin effector halorhodopsin (eNpHR3.0) selectively in VTA GABA neurons. An increase in DA neuron activity during a 2-s amber light activation was observed (fig. S2). We conclude that NAc D1R-MSNs suppress the tonic activity of VTA GABA neurons, which disinhibits VTA DA neurons.

With addictive drugs, it is generally assumed that disinhibition is fully reversed once the drugs are eliminated. We hypothesized that the disinhibitory circuit in the VTA may undergo persistent remodeling with repetitive drug exposure. We investigated whether the synapse between D1-MSNs and VTA GABA neurons is capable of expressing activity-dependent synaptic plasticity. We elicited GABA release from axonal terminals in the VTA with blue light and recorded from VTA GABA neurons (Fig. 2A). High-frequency stimulation (HFS; Fig. 2A) of MSN terminals led to a robust potentiation of light-evoked IPSCs ($183 \pm 22\%$ of baseline, $n = 15$, $P < 0.05$; Fig. 2B). This inhibitory long-term potentiation (iLTP), which could also be induced with low Cl⁻-containing internal solution ($135 \pm 8\%$ of baseline, $n = 8$, $P < 0.01$; fig. S3A), was associated with a decrease of the failure rate (baseline, 0.29 ± 0.07 ; after HFS, 0.2 ± 0.06 ; $n = 12$, $P < 0.01$) and changed variance ($1/CV^2$; baseline, 2.02 ± 0.54 ; after HFS, 4.23 ± 1.26 ; $n = 15$, $P < 0.01$); the reduction of the paired pulse

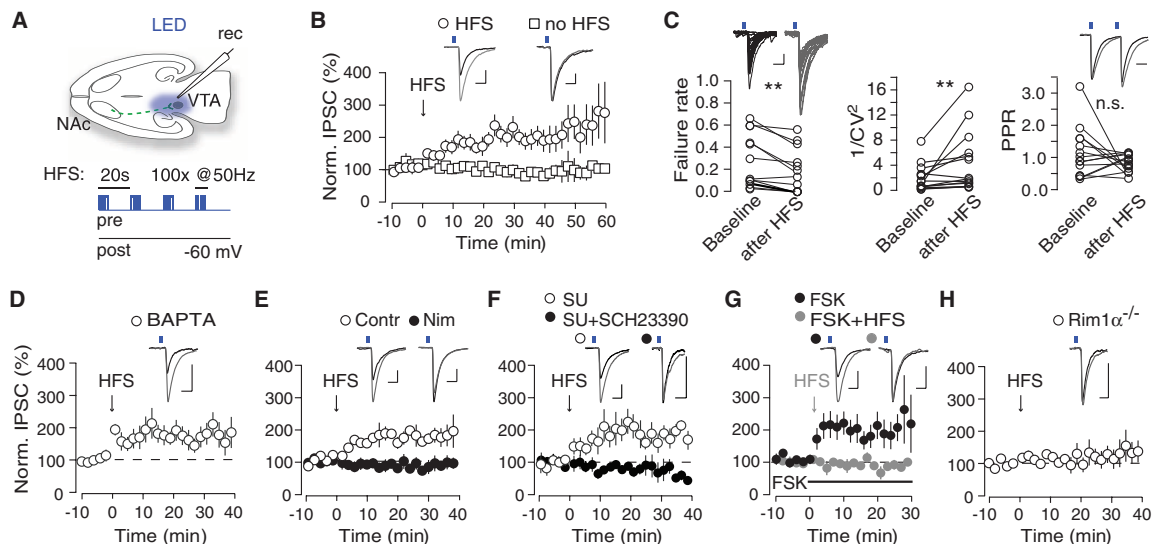
ratio (PPR) was not significant because of a high variance (baseline, 1.02 ± 0.19 ; after HFS, 0.93 ± 0.08 ; $n = 15$, $P > 0.05$; Fig. 2C). The three parameters in combination strongly suggest an increase in release probability. Infusion of a high concentration of the calcium chelator BAPTA (10 mM) into the postsynaptic neuron did not block iLTP ($160 \pm 20\%$ of baseline, $n = 14$, $P < 0.01$; Fig. 2D), whereas the calcium channel blocker nimodipine applied extracellularly (Nim, 10 μ M) or blockade of D1Rs abolished the potentiation ($91 \pm 18\%$ and $92 \pm 10\%$ of baseline, $n = 7$ and 7 , $P > 0.05$; Fig. 2, E and F).

Presynaptic forms of synaptic plasticity depend on the cyclic adenosine monophosphate-protein kinase A (cAMP-PKA) cascade (14). We aimed to stimulate potentiation with the adenylyl cyclase (AC) activator forskolin (FSK, 10 μ M). This caused a potentiation of the transmission ($178 \pm 32\%$ of baseline, $n = 11$, $P < 0.01$; Fig. 2G, black trace), which occluded the ability of HFS to induce iLTP ($86 \pm 6\%$ of baseline, $n = 4$, $P > 0.05$; Fig. 2G, gray trace). The underlying mechanism therefore likely involves this cascade in the terminals of NAc MSNs initiated by D1Rs. We confirmed that FSK-induced potentiation is solely mediated by presynaptic PKA by additionally loading the postsynaptic cell with the membrane-impermeable PKA inhibitor PKI 6-22 (20 μ M) while bath-applying FSK (fig. S3B). Taken together, induction as well as expression of iLTP is likely to be presynaptic, akin to well-described forms of potentiation at hippocampus mossy fiber excitatory synapses (15). Because this “sister” LTP requires the scaffolding protein Rim1 α (16), we tested its involvement in iLTP. HFS in the Rim1 α ^{-/-} mice left basal IPSC amplitudes unaffected ($97 \pm 14\%$ of baseline, $n = 7$, $P > 0.05$; Fig. 2H). Hence, iLTP in the VTA also depends on presynaptic Rim1 α .

We next wanted to test whether inhibitory transmission between D1R-MSNs and VTA

Fig. 2. HFS induces cAMP-PKA-dependent iLTP.

(A) Setup: Whole-cell recordings of light-evoked IPSCs from VTA neurons and induction protocol. (B) HFS of MSN terminals elicits iLTP. (C) Group data for failure rate, coefficient of variation ($1/CV^2$), and paired pulse ratio (PPR) at baseline and after HFS. (D and E) Intracellular BAPTA blocked iLTP (D) in contrast to bath-applied nimodipine (Nim) (E). (F) SCH23390 and sulpiride (SU) blocked iLTP. (G) FSK potentiated IPSC amplitudes and occluded iLTP. (H) No iLTP in Rim1 α ^{-/-} mice. All insets: Example traces of IPSCs at baseline (black) and after HFS (gray). Scale bars, 100 pA, 10 ms, except for (F), 40 pA, 10 ms. Data are means \pm SEM.



GABA neurons was affected by repetitive drug exposure. Cocaine is a highly addictive drug that evokes synaptic plasticity at several excitatory synapses of the mesolimbic system (17). Its reinforcing effects are mediated by increasing DA concentration in the NAc instead of disinhibiting DA neurons [cocaine actually briefly inhibits DA neuron firing in the acute phase (18)]. To test for cocaine-induced synaptic plasticity at this disinhibitory circuit, we repeatedly treated mice with cocaine [15 mg/kg intraperitoneally (i.p.) for 5 days; Fig. 3A], prepared midbrain slices 24 hours after the last injection, and examined whether this treatment interfered with the ability to elicit iLTP. Drug exposure disrupted HFS-induced iLTP (saline, $157 \pm 29\%$ of baseline, $n = 9$; cocaine, $86 \pm 7\%$ of baseline, $n = 9$; $P < 0.05$; Fig. 3B) and was associated with a decrease of the PPR (saline, 1.28 ± 0.09 , $n = 27$; cocaine, 0.82 ± 0.09 , $n = 19$; $P < 0.01$; Fig. 3C), indicating an occlusion scenario. Bath application of FSK readily potentiated light-evoked IPSCs in slices from saline-treated animals, whereas it failed to potentiate the IPSCs in the cocaine group (saline, $249 \pm 51\%$ of baseline, $n = 9$; cocaine, $101 \pm 15\%$ of baseline, $n = 8$; $P < 0.05$; Fig. 3D), confirming the involvement of the cAMP-PKA cascade in the induction of cocaine-evoked synaptic plasticity (19).

To test whether induction of cocaine-evoked inhibitory plasticity was dependent on the increase of extracellular DA concentration, we exposed mice carrying a mutated cocaine-insensitive DAT (DAT_{KI}) (20) repeatedly to cocaine. In DAT_{KI} mice, cocaine treatment did not disrupt the ex vivo iLTP ($223 \pm 38\%$ of baseline, $n = 12$, $P < 0.05$), whereas potentiation was not fully induced in heterozygous littermates ($126 \pm 23\%$ of baseline, $n = 7$, $P > 0.05$; Fig. 3E). This indicates that without DAT inhibition, cocaine does not disrupt iLTP, thus confirming that in vivo cocaine-evoked synaptic plasticity is induced by a dopamine-dependent mechanism.

The decreased PPR values suggested an enhanced GABA release probability at DIR-MSN terminals after cocaine treatment. We thus recorded spontaneous inhibitory synaptic currents (sIPSCs) after repeated cocaine treatment (Fig. 3, F to H). Cocaine increased the sIPSC frequency in GABA neurons (saline, 7.1 ± 1.1 Hz, $n = 11$; cocaine, 16.2 ± 4.1 Hz, $n = 12$, $P < 0.05$, with a trailing enhancement of the amplitudes: saline, 56 ± 5.1 pA, $n = 11$; cocaine, 72.6 ± 11 pA, $n = 12$; $P > 0.05$; Fig. 3, F and G) but not in DA neurons, where the frequency of sIPSC was in fact lower in slices from cocaine-treated mice (frequencies: saline, 14.7 ± 2.5 Hz, $n = 11$; cocaine, 7.4 ± 1.4 Hz, $n = 10$; $P < 0.05$; amplitudes: saline,

47.1 ± 3.3 pA, $n = 11$; cocaine, 40.5 ± 2.1 pA, $n = 10$; Fig. 3, F and H), in line with a depressed inhibition reported previously (21, 22). Our data suggest a long-lasting disinhibition of VTA DA neurons, most likely through the potentiation of inhibitory synaptic transmission onto GABA neurons through a presynaptic mechanism. If this is the case, then the basal firing activity of VTA DA neurons should be increased after repeated cocaine treatment. Indeed, DA neurons showed increased spiking and burst firing activity after repeated cocaine treatment relative to saline-injected mice [saline, 3.4 ± 0.6 Hz and $24.7 \pm 5.7\%$ spikes fired in bursts (SIB), $n = 23$; cocaine, 9.0 ± 1.7 Hz and $53.1 \pm 8.9\%$ SIB, $n = 16$; $P < 0.01$ and $P < 0.005$; Fig. 3I and fig. S4], whereas GABA neurons fired at lower rates after cocaine (saline, 9.9 ± 2.1 Hz, $n = 20$; cocaine, 5.1 ± 1 Hz, $n = 15$; $P < 0.05$; Fig. 3I). Elevated firing activity of DA neurons is unlikely to result from increased direct excitation onto these cells, because one single injection of cocaine, which increases glutamatergic tone onto DA neurons (23), failed to increase firing rates of DA neurons 24 hours after the injection (fig. S5). Taken together, these findings imply that cocaine selectively potentiates GABA release from NAc DIR-MSN terminals in a DA-dependent fashion such that VTA DA neurons are tonically disinhibited in the long run.

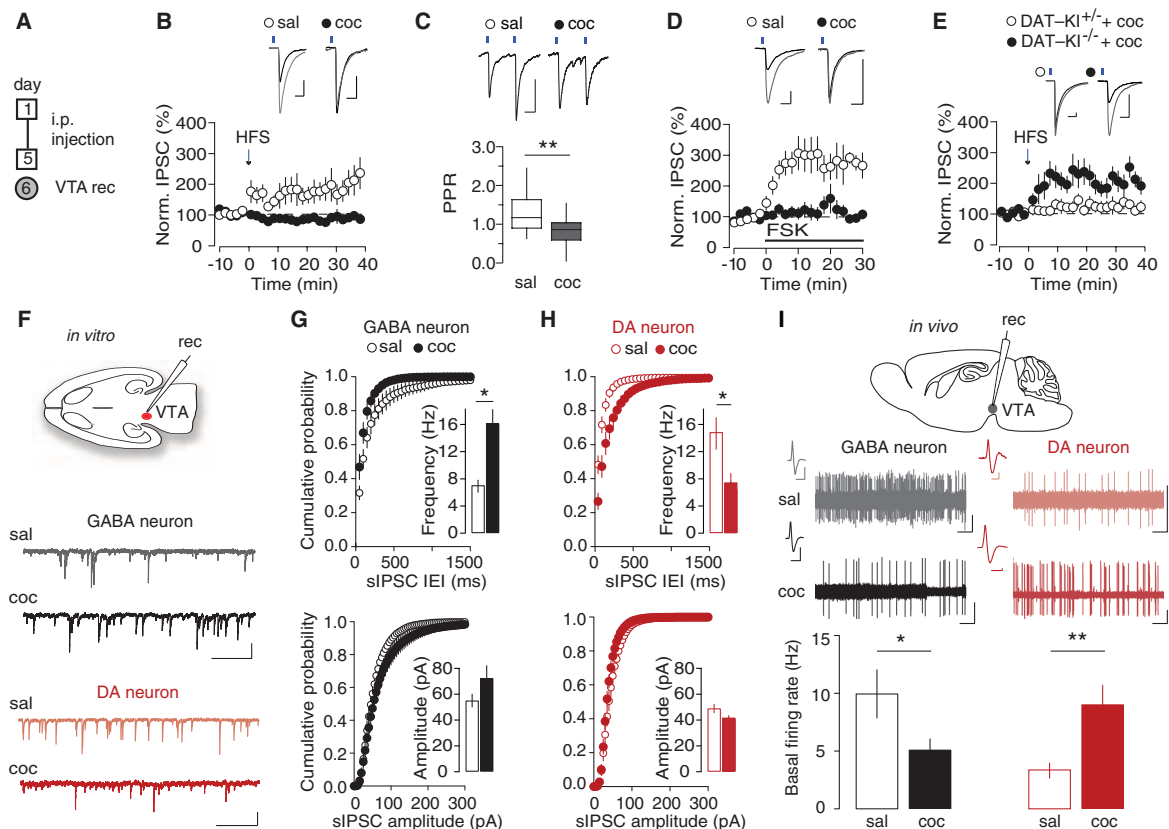


Fig. 3. Potentiation of inhibitory transmission by cocaine. (A) Treatment protocol. (B) Cocaine treatment abolishes iLTP. Scale bars, 100 pA, 10 ms. (C) PPR example traces and group data. Scale bars, 20 ms, 50 pA. (D) Occlusion of FSK potentiation by cocaine treatment. Scale bars, 100 pA, 10 ms. (E) Failure to abolish iLTP in DAT_{KI} mice. Scale bars, 100 pA, 10 ms. (F) Setup and example

traces of sIPSCs. Scale bars, 50 pA, 0.5 s. (G and H) Cumulative probability distributions of sIPSC in GABA neurons (G) and DA neurons (H). Insets: bar graphs with means \pm SEM. (I) Setup and example traces from in vivo recordings of VTA GABA and DA neurons (scale bars, 2 s, 10 mV; inset scale bars, GABA, 2 ms, 10 mV; DA, 2 ms, 2 mV). Bottom: Group data for firing rates.

How may drug-evoked inhibitory plasticity relate to behavioral actions of cocaine caused by the activation of DIR-MSNs (24)? We assessed locomotor sensitization (Fig. 4A), a model for incentive saliency of cocaine that develops over five daily injections, just as cocaine-evoked inhibitory plasticity (25). We first verified the consequences of the iLTP induction protocol in vivo on the activity of VTA neurons (Fig. 4A) and observed inversed firing frequencies in GABA and DA neurons (GABA HFS versus no HFS, 2.5 ± 1 Hz and 13 ± 2 Hz, $P < 0.0001$; DA HFS versus no HFS, 9.5 ± 6 Hz and 3 ± 1 Hz, $P < 0.01$; 35 ± 12 SIB versus $16 \pm 4\%$ SIB, $P < 0.05$; $n = 10$ to 17; Fig. 4B and fig. S4), comparable to the cocaine treatment. On subsequent days, locomotor sensitization to cocaine was enhanced (control AAV, 1389 ± 184 turns/hour, $n = 15$; ChR2-AAV, 3104 ± 555 turns/hour, $n = 11$; $P < 0.01$; Fig. 4C). We next tested the effect of an in vivo HFS on conditioned place preference (CPP), a paradigm to measure the memory effect of drug reward (26). HFS was applied outside the conditioning chamber 1 day before the drug administration (10 mg/kg), which prevented CPP (control AAV, 105 ± 29 min, $n = 9$; ChR2-AAV, 17 ± 27 , $n = 11$; $P < 0.05$; Fig. 4D). These data support a model whereby the VTA serves as a gate for downstream circuit adaptations that un-

derlie sensitization and occludes CPP where cue association requires burst activity of DA neurons.

The cellular correlate of the disinhibition of VTA DA neurons is a form of homosynaptic potentiation of GABA transmission onto VTA GABA neurons. This cocaine-evoked inhibitory plasticity is DA-dependent and is expressed presynaptically. As a consequence, VTA DA neurons fire at higher frequencies, which facilitates the induction of locomotor sensitization and occludes CPP. This adaptation of the inhibitory limb of the mesolimbic circuitry occurs in parallel with a strengthening of excitatory afferents onto DA neurons in the VTA (23, 27, 28). Then, after several days of withdrawal, excitatory transmission in the NAc also adapts (26). Thus, the drug-evoked synaptic plasticity in back-projecting DIR-MSNs, described in the present study, emerges as a crucial step in circuit remodeling (29). Note that DIR-MSNs undergo presynaptic and postsynaptic changes (30), resulting in an overall strengthening of their inhibitory effects and enhanced locomotor sensitization, whereas inhibition of DIR-MSNs attenuates this behavior (31).

Drug-evoked inhibitory plasticity may also prevent further associative learning and may lead to behavioral adaptations such as compulsive cocaine seeking or incubation of craving (32, 33). Clearly, a picture is emerging of mesolimbic cir-

cuit remodeling that affects excitatory as well as inhibitory transmission, with the effect of enhancing DIR-MSN function. Controlling the activity of the DIR-MSNs, by pharmacological means or neuromodulation, may therefore emerge as an appealing target for novel therapeutic interventions in addiction.

References and Notes

1. J. J. Letzkus *et al.*, *Nature* **480**, 331–335 (2011).
2. F. Gambino, A. Holtmaat, *Neuron* **75**, 490–502 (2012).
3. R. C. Froemke, M. M. Merzenich, C. E. Schreiner, *Nature* **450**, 425–429 (2007).
4. S. W. Johnson, R. A. North, *J. Neurosci.* **12**, 483–488 (1992).
5. K. R. Tan *et al.*, *Nature* **463**, 769–774 (2010).
6. H. G. Cruz *et al.*, *Nat. Neurosci.* **7**, 153–159 (2004).
7. J. Bertran-Gonzalez *et al.*, *J. Neurosci.* **28**, 5671–5685 (2008).
8. S. R. Sesack, A. A. Grace, *Neuropsychopharmacology* **35**, 27–47 (2010).
9. Y. Xia *et al.*, *J. Neurosci.* **31**, 7811–7816 (2011).
10. M. Watabe-Uchida, L. Zhu, S. K. Ogawa, A. Vamanrao, N. Uchida, *Neuron* **74**, 858–873 (2012).
11. G. Nagel *et al.*, *Curr. Biol.* **15**, 2279–2284 (2005).
12. M. P. Smidt *et al.*, *Proc. Natl. Acad. Sci. U.S.A.* **94**, 13305–13310 (1997).
13. K. R. Tan *et al.*, *Neuron* **73**, 1173–1183 (2012).
14. M. G. Weiskopf, P. E. Castillo, R. A. Zalutsky, R. A. Nicoll, *Science* **265**, 1878–1882 (1994).
15. P. E. Castillo, *Cold Spring Harb. Perspect. Biol.* **4**, a005728 (2012).
16. P. E. Castillo, S. Schoch, F. Schmitz, T. C. Südhof, R. C. Malenka, *Nature* **415**, 327–330 (2002).
17. C. Lüscher, R. C. Malenka, *Neuron* **69**, 650–663 (2011).
18. M. S. Brodie, T. V. Dunwiddie, *Naunyn Schmiedeberg Arch. Pharmacol.* **342**, 660–665 (1990).
19. D. W. Self *et al.*, *J. Neurosci.* **18**, 1848–1859 (1998).
20. R. Chen *et al.*, *Proc. Natl. Acad. Sci. U.S.A.* **103**, 9333–9338 (2006).
21. B. Pan, C. J. Hillard, Q.-S. Liu, *J. Neurosci.* **28**, 1385–1397 (2008).
22. Q.-S. Liu, L. Pu, M.-M. Poo, *Nature* **437**, 1027–1031 (2005).
23. M. A. Ungless, J. L. Whistler, R. C. Malenka, A. Bonci, *Nature* **411**, 583–587 (2001).
24. M. K. Lobo *et al.*, *Science* **330**, 385–390 (2010).
25. T. E. Robinson, K. C. Berridge, *Brain Res. Brain Res. Rev.* **18**, 247–291 (1993).
26. H. L. Fields, G. O. Hjelmstad, E. B. Margolis, S. M. Nicola, *Annu. Rev. Neurosci.* **30**, 289–316 (2007).
27. C. Bellone, C. Lüscher, *Nat. Neurosci.* **9**, 636–641 (2006).
28. M. T. C. Brown *et al.*, *PLoS ONE* **5**, e15870 (2010).
29. D. Belin, B. J. Everitt, *Neuron* **57**, 432–441 (2008).
30. V. Pascoli, M. Turiault, C. Lüscher, *Nature* **481**, 71–75 (2012).
31. R. Chandra *et al.*, *Front. Mol. Neurosci.* **6**, 13 (2013).
32. J. W. Grimm, B. T. Hope, R. A. Wise, Y. Shaham, *Nature* **412**, 141–142 (2001).
33. M. Mamei *et al.*, *Nat. Neurosci.* **12**, 1036–1041 (2009).

Acknowledgments: We thank M. Serafin and the members of the Lüscher laboratory for suggestions on the manuscript, M. Brown for support during the in vivo electrophysiology experiments, G. Miesenböck for GADCre mice, and S. Schoch for Rim1α^{-/-} mice. Supported by the Swiss National Science Foundation, the European Research Council, and “Synapsy,” a National Competence Center in Research (C.L.) and by a Swiss Confederation scholarship (J.C.Y.W.).

Supplementary Materials

www.sciencemag.org/content/341/6153/1521/suppl/DC1
Materials and Methods
Figs. S1 to S5

26 February 2013; accepted 5 September 2013
10.1126/science.1237059

Fig. 4. In vivo HFS enhances cocaine-induced locomotor sensitization and occludes conditioned place preference. (A) Experimental setup. (B) Example traces of in vivo recordings of VTA GABA and DA neurons (scale bars, 5 mV; inset scale bars, 2 ms, 10 mV). Bottom: Group data for firing rates. (C) Locomotor activity immediately after saline (days –3 to –1) or cocaine (days 1 to 5) injections (i.p.). (D) Group data for CPP score. Data are means \pm SEM.

